diffusion-fundamentals.org

The Open-Access Journal for the Basic Principles of Diffusion Theory, Experiment and Application

3D X-ray CT and diffusion measurements to assess tortuosity and constrictivity in a sedimentary rock

Hiroaki Takahashi, Yoshimi Seida, Mikazu Yui

Geological Isolation Research and Development Unit, Japan Atomic Energy Agency, Japan

Corresponding author:
Hiroaki Takahashi
Geological Isolation Research and Development Unit
Japan Atomic Energy Agency
4-33, Muramatsu, Tokai-mura, Naka-gun, Ibaraki 319-1194
E-Mail: takahashi.hiroaki@jaea.go.jp

Abstract

A high-resolution, three-dimensional (3D) image of the interior of the sedimentary rock was obtained by means of nano-focus X-ray computer tomography (X-ray CT). Using computational methods to analyze the 3D microstructure of the rock, we presented the tortuosity and geometrical constrictivity. We also presented results on the tritiated water (HTO) diffusion tests and a mercury intrusion porosimetry (MIP) test performed on the rock. We have compared these results to understand the dominant parameters that control diffusion of HTO in the present system. These results suggest that the dominant parameters in the present system are not the constrictivity but the tortuosity and the diffusion-accessible porosity. The material considered in this study is the siliceous mudstones sampled from 500 m in depth at the Wakkanai formation around Horonobe underground research center in Hokkaido, Japan.

Keywords

diffusion, tortuosity, constrictivity, nano-focus X-ray CT, siliceous mudstones, tritiated water, transport of radionuclides, mercury intrusion porosimetry

1. Introduction

The siliceous mudstones of the Wakkanai formation at the Horonobe underground research center are studied to investigate the transport behaviour of radionuclides. Horonobe underground research center is a generic underground laboratory for a high-level radioactive waste disposal, not for a repository. The transport of radionuclides through the low permeable siliceous mudstone matrix is a diffusion-controlled process. The geometrical properties of pore space and connectivity for radionuclides migration in natural rocks is one of key factors for performance assessment in deep geological disposal system of high-level radioactive waste. For the assessment, there is a need to predict through model for the effect of the pore structure radionuclides migration.

The effective diffusion coefficient, D_e, defined by $D_e = \varphi\delta/\tau^2 \times D_w$ (φ: diffusion-accessible (or effective) porosity for the solute, δ: constrictivity, τ: tortuosity, D_w: diffusion coefficient of ions in free water) [1]. Fig. 1 shows definitions of tortuosity [2] and constrictivity, δ [3] as geometrical parameters. The δ is only important if the size of the solute becomes comparable to the size of the pore [1]. The φ accounts for the reduced cross-sectional area available for diffusion in the pore space (φ equals the overall porosity, if the total pore space in isotropic media is available for the diffusion process) [1]. The φ can be experimentally obtained from the steady-state breakthrough behavior of non-sorbing ion. The τ and the δ are used as adjustable parameters in conventional models of radionuclides migration in porous media, because it is difficult to measure these factors directly. The direct measurement of those factors in relation to the real pore structure of the siliceous mudstones has not been performed so far.

In order to obtain 3D representation of the rock pore space nondestructively, micro X-ray computer tomography (X-ray CT) scanning is a powerful tool. This approach provides a direct description of the pore space, but was limited by the machine resolution - till lately a few microns. Recently, CT scanning has been improved to be able to describe the sub-micron sized features present in many siliceous mudstone samples. High-resolution, three-dimensional images of the interior of porous media systems can be obtained. Accordingly, methods are needed to directly convert the pore structure to a network structure.

In the last 10 years, there has been a surge of interest in network extraction simulated by the availability of micro-CT images. The first rigorous method to extract networks was developed by Lindquist and Lee [4], Lindquist and Venkatarangan [5] using an algorithm that defined the medial axis of the pore space.

In the present study, direct observation of the macro-pore geometry, their distribution and their connectivity in the siliceous mudstones were performed by means of nano-focus X-ray CT to identify real tortuosity and geometrical constrictivity by applying a medial-axis-based technique [4,5]. In addition, a comparison of the results with properties of pore space obtained from a set of HTO through-diffusion tests and a mercury intrusion porosimetry (MIP) test was performed on the rock samples obtained from vicinal location.

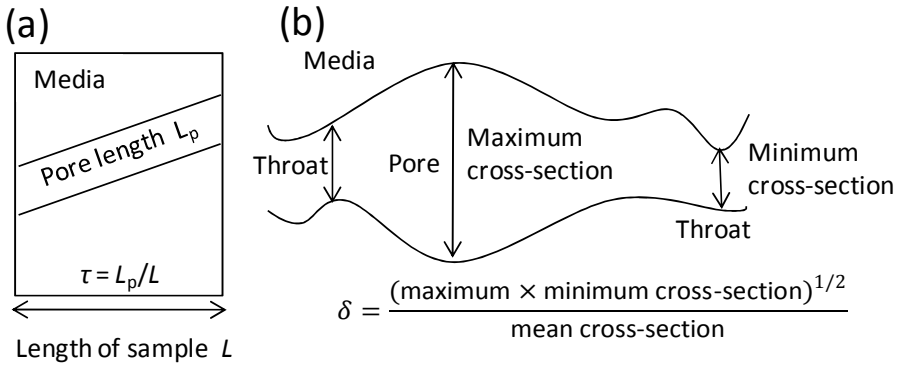

Fig. 1. Definitions of (a) tortuosity and (b) constrictivity.

diffusion-fundamentals.org 11 (2009) 89, pp 1-11

Table 1 Pore-water compositions used in this study.

Ion strength (eq dm^{-3})	pH	[Na^+] (mol dm^{-3})	[K^+] (mol dm^{-3})	[Li^+] (mol dm^{-3})	[Ca^+] (mol dm^{-3})	[Mg^{2+}] (mol dm^{-3})	[HCO_3^-] (mol dm^{-3})	[SO_4^{2-}] (mol dm^{-3})	[Cl^-] (mol dm^{-3})
0.227	8.2	0.207	0.0025	0.00245	0.0021	0.00576	0.0162	0.00115	0.209

2. Experimantal methods

The material considered in this study is the siliceous mudstones sampled from 500 m in depth at the Wakkanai formation around Horonobe underground research center.

A MIP test was used to determine the connected (or open) porosity and to obtain information on the pore-throat size distribution in a dry condition. This test is based on the intrusion (and extrusion) of a non-wetting fluid (mercury) into the dried and degassed sample cores by increasing (and, respectively, decreasing) the applied mercury pressure. Bulk 5×5×5 mm^3 samples with no apparent cracks or fissures were measured with Micromeritics Autopore IV 9520 mercury porosimeter.

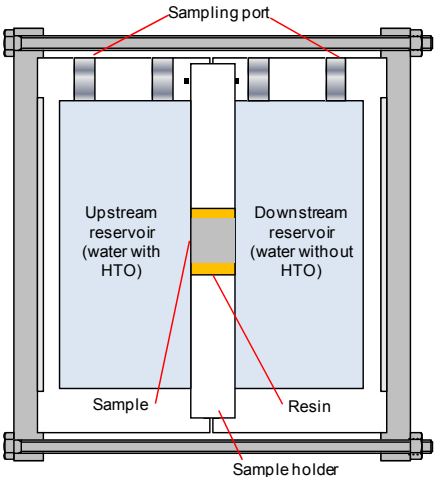

Fig. 2. Experimental set-up for through-diffusion experiment (not to scale).

The effective diffusion coefficient, D_e, of HTO and the diffusion-accessible porosity, φ, were measured by through-diffusion tests with constant concentration in the inlet reservoir. The experiments were performed with 20-mm-diameter and 20-mm- thicknesses samples for horizontal and vertical direction in the Wakkanai formation. HTO diffusion experiments were conducted under the argon atmospheric condition (O_2 < 10ppm) with synthetic water of a composition as close as possible to the pore-water composition of the formation given by Table 1. Fig. 2 schematically represents the diffusion cells used in this study. The through-diffusion cells comprise two reservoirs of equal size and volume (100 cm^3), a sample holder and the whole being sealed with resin and screwed together. Results were analyzed by fitting the total diffused radioactivity, according to the method known as the "time-lag method" [6]. A linear regression analysis of the data on the total accumulated radioactivity versus time is performed and D_e and φ are derived, respectively. The δ/τ^2 estimated from the values of D_e, φ and D_w. The D_w value for HTO is taken to be 2.44 × 10^{-9} m^2 s^{-1} [7] at 25°C.

An about 300 μm diameter and length specimen was prepared from larger siliceous mudstones. The specimen was imaged at 270 nm voxel resolution by means of the nano-focus X-ray CT (SkyScan-2011). The CT measurement was performed with setting Z axis of sample along vertical direction in the Wakkanai formation. The high-resolution, 3D image was processed by using the software package Exfact Analysis for Porous/Particles (Nihon Visual Science, Inc.) to directly convert the pore structure to a network structure. We determined geometrical path tortuosity and radii of pore, r_p, and throat, r_t by the processing. Constrictivity, δ [3], was determined from equation (1) using

the r_p and the r_t assuming that mean cross-section could be evaluated by linear approximation with average of maximum and minimum cross-section.

$$\delta = \frac{(\text{maximum} \times \text{minimum cross-section})^{\frac{1}{2}}}{\text{mean cross-section}} = \frac{\left(\pi r_p^2 \times \pi r_t^2\right)^{\frac{1}{2}}}{\left(\frac{\pi r_p^2 + \pi r_t^2}{2}\right)} \qquad (1)$$

3. Results and Discussion

Fig. 3 shows a result of the MIP test for the siliceous mudstones. In fact the method does not measure effective pore size but rather the effective radii of pore -entry (i.e. throat) sizes. The connected porosity obtained from intrusion curve was 0.33. The hysterisis evident in the cumulative curves (Fig. 3a) indicates that 36.2% of the intruded mercury volume is trapped within the pore network after the extrusion stage. This is mainly due to the pore network complexity. Intrusion fills all the accessible and interconnected pore space, giving the distribution of total porosity, whereas on the complete release of the intrusion pressure it will let only some mercury out from the nonconstricted pores [8]. The nonconstricted pores will be main diffusion path which directly affects accessibility of radionuclides and will contribute the diffusivity significantly.

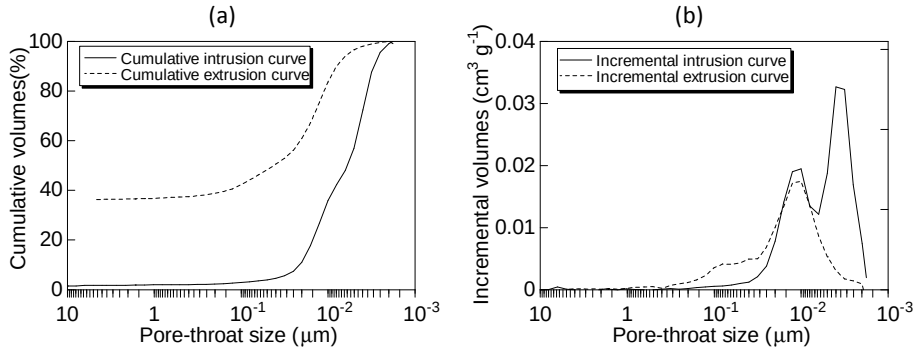

Fig. 3. The estimation of pore space characteristics for the siliceous mudstone using MIP curves. (a) Cumulative volume curves. (b) Incremental volume curves.

Table 2 Accessible porosity, effective diffusion coefficient and the δ/τ^2 obtained from HTO diffusion experiments.

Direction to the ground	φ	D_e (m^2 s^{-1})	δ/τ^2
Vertical	0.19	8.80×10^{-11}	0.19
Horizontal	0.22	1.02×10^{-10}	0.19

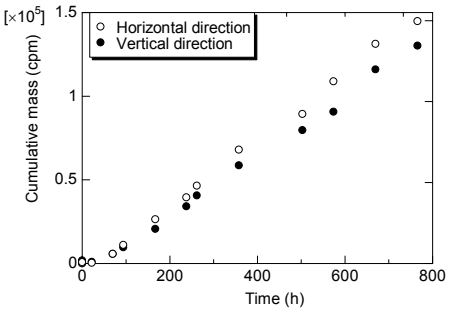

Fig. 4. Cumulated radioactivity in the downstream compartment of HTO through siliceous mudstones of the Wakkanai formation. Vertical (○) and horizontal (●) direction to the ground.

Fig. 4 shows experimental results of through-diffusion tests of HTO through siliceous mudstones of the Wakkanai formation. Table 2 shows D_e, φ and the δ/τ^2 obtained from the HTO diffusion experiments. The φ obtained from HTO diffusion experiments were close values with the porosity, 0.21 that corresponds to only some mercury out from the nonconstricted pores on the complete release of the intrusion pressure. This indicated main HTO diffusion paths were the nonconstricted (nontrapped) pores. The δ/τ^2 for vertical direction was 0.19 same as horizontal direction. On the contrary, D_e and φ for vertical direction were a little bit smaller than their values for horizontal direction . These results correlated to the geometrical properties of pore space and connectivity obtained by 3D image analysis as follows.

Fig. 5 (a) shows 3D image of siliceous mudstone of the Wakkanai formation used in this analysis at the size of 138.24 μm, taken at a resolution of 270 nm (512^3 voxels). Clausnitzer and Hopmans [9] found that the side length of a representative elementary volume (REV) was approximately 5.15 times the bead diameter for a mono-size bead system. For the system, the image size is 512^3 voxels, this is equivalent to a side length 512 pixel and 138.24 μm at resolution of 270 nm. The ratio of the side length of the image obtained to the particle diameter (1 to 10 μm) from the SEM observation (see Fig. 6) is larger than 5.15, an REV is obtained due to the non-uniformity of the system. Fig. 5 (b) shows a cross-sectional image of the 3D image. The voxel intensity increases with increasing density and atomic number of the minerals. Fe-bearing strong X-ray absorbers like pyrite are blight, some clay minerals are dark, air-filled pores are the darkest in the image. Fig. 5 (c) and (d) show 3D image and a slice of center of Z axis after segmentation for pore-network extraction, respectively. Fig. 7 (a) and (b) shows 3D image of medial axis and throats generated from the extracted pore-network 3D image, respectively. Once pore and throat locations and sizes have been determined, other pore network properties can be found. A total of 4,527 pores and 10,455 throats were identified.

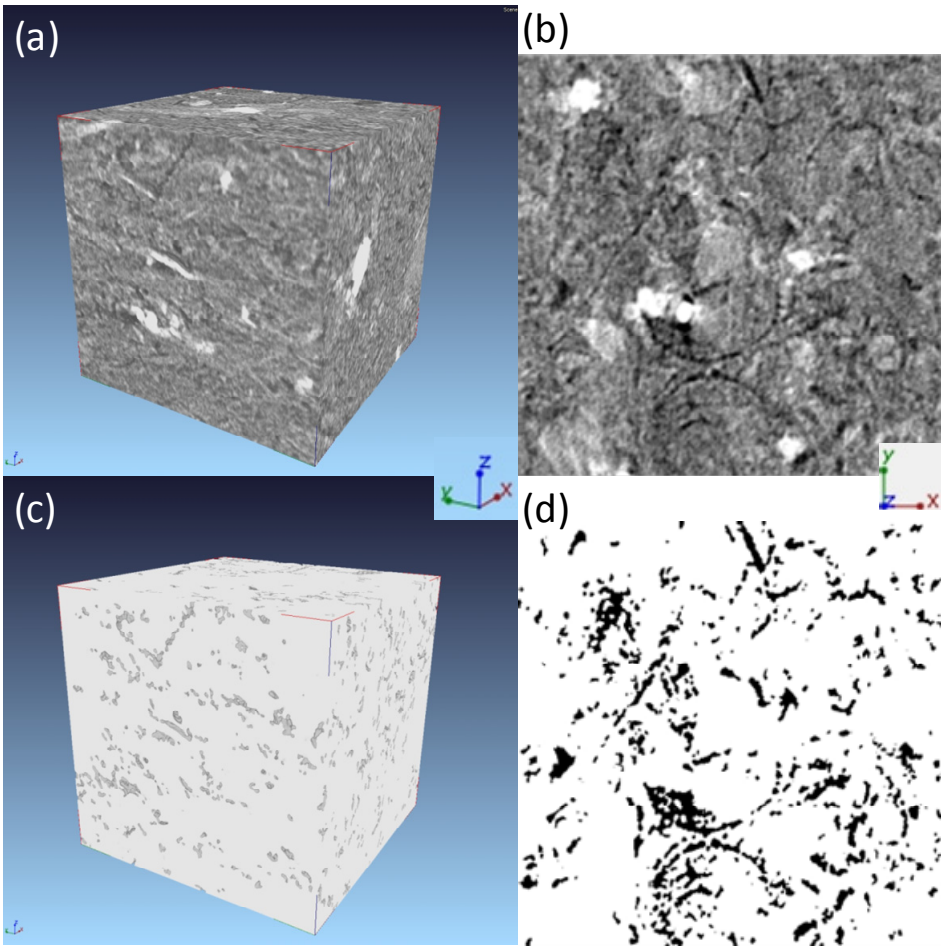

Fig. 5. (a) Three-dimensional image (512^3 with a voxel size of 270 nm) of siliceous mudstone of the Wakkanai formation and (b) a slice of center of Z axis. (c) Three-dimensional image after segmentation (dark gray areas denote pore spaces) and (d) a slice of center of Z axis (black areas denote pore spaces).

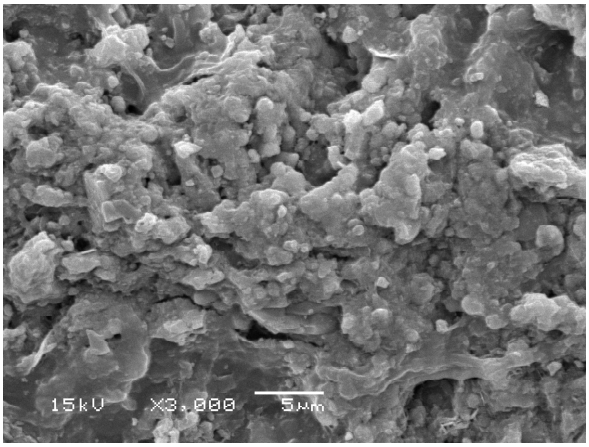

Fig. 6. Two-dimensional SEM image of the siliceous mudstones of the Wakkanai formation.

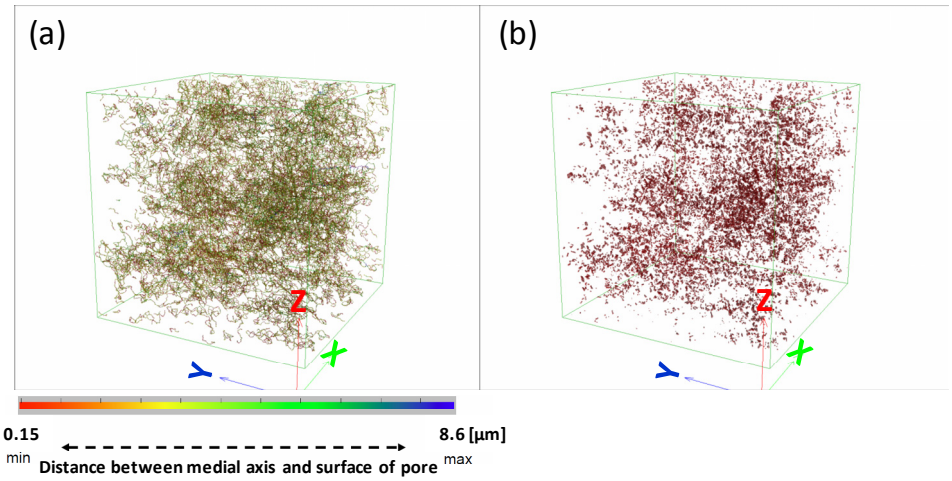

Fig. 7. Three-dimensional image of (a) medial axis and (b) throats of the siliceous mudstone of the Wakkanai formation used in this study.

Table 3 shows network properties of medial axis for the siliceous mudstones. In the case of the Z direction, 33 starting side medial axis locations, 123 ending side medial axis locations and 20/33 start face voxels connected to end face. The number of start face voxels connected to end face to the Z direction was less than the one to other directions. This result was consistent with the results from the diffusion experiments that the φ for vertical direction was smaller than their values for horizontal direction as shown in Table 2. This agreement indicated that the number of effective diffusion path controlled diffusion of HTO in this system.

Fig. 8 shows distributions of pore radii, throat radii and effective throat/pore radius ratio of the sample and these averages were 1.72 μm, 0.55 μm and 0.265, respectively. These results showed that extracted pore network was including sub-micron sized features.

Fig. 9 shows the τ distributions of X, Y and Z directions and the δ distributions in the siliceous mudstone. The average of τ distributions in the X, Y and Z directions were 2.94, 2.18 and 2.64, respectively. The average of X and Y directions and the average of the three directions were estimated at 2.56 and 2.59, respectively. Here, the τ for X and Y directions correspond to horizontal direction and the Z direction corresponds to vertical direction. The τ estimated form 3D image analysis was roughly isotopic for vertical and horizontal directions. This was consistent with the δ/τ^2 obtained from HTO diffusion experiments for vertical and horizontal direction. The average of the constrictivity was estimated at 0.47. The value of δ/τ^2, 0.19 obtained from HTO diffusion experiment was closer value with $1/\tau^2$, 0.15 than δ/τ^2, 0.07 estimated from 3D image analysis. It indicated that the δ could be neglected and the HTO-diffusion-accessible pore sizes of the siliceous mudstone investigated here were much bigger than the HTO size. These results indicated that the geometrical structure of HTO diffusion path was similar to the one measured by X-ray CT and the dominant parameters that control diffusion of HTO in present system are the φ and the τ.

Table 3 Network properties of medial axis for the siliceous mudstones of the Wakkanai formation.

Direction to the ground	Direction	Starting side medial axis locations	Ending side medial axis locations	Starting face voxels connected to end face	Average of τ
Vertical	Z	33	123	20	2.64
Horizontal	Y	189	43	152	2.18
Horizontal	X	62	303	55	2.94

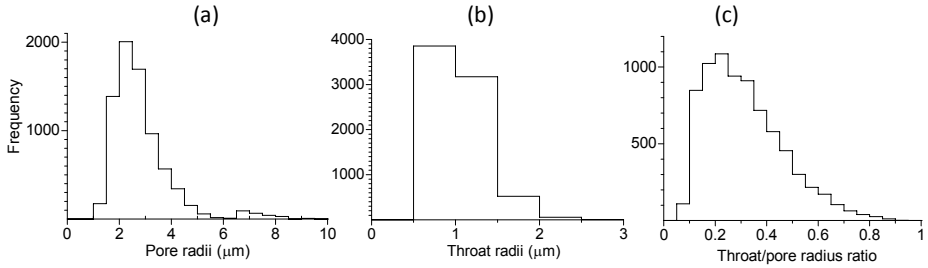

Fig. 8 Distributions of (a) pore radius, (b) throat radius and (c) effective throat/pore radius ratio of the siliceous mudstone.

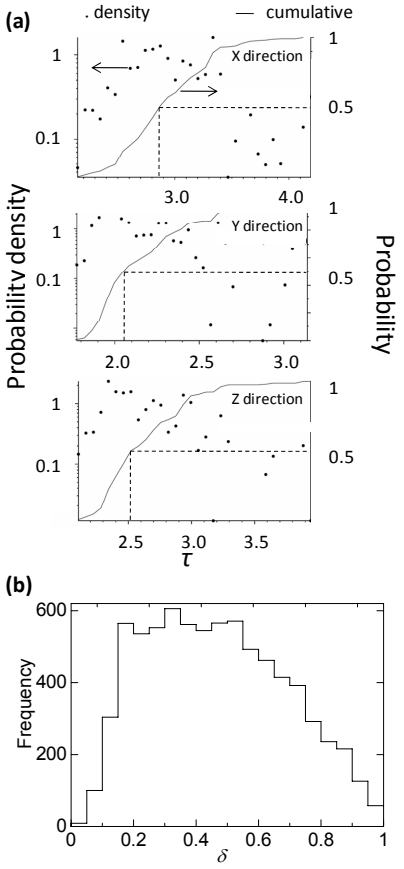

Fig. 9 (a) The τ distributions of X, Y and Z directions, (b) the δ distributions in the siliceous mudstone.

4. Conclusion.

This study has been conducted to directly observe pore geometry, their distribution and their connectivity in the siliceous mudstones by means of nano-focus X-ray CT to identify real tortuosity and constrictivity of the rock and to compare the results with the geometrical factors and porosities obtained from a set of HTO through-diffusion tests and a MIP test performed on the rock. We concluded based on this study as follows.

1) The φ obtained from HTO diffusion experiments was close to the porosity that corresponds to only some mercury out from the nonconstricted pores on the complete release of the intrusion pressure. This indicated main HTO diffusion path was the nonconstricted (nontrapped) pore.
2) There was a good agreement between the δ/τ^2 obtained from HTO diffusion experiments for vertical direction in the Wakkanai formation and the one for horizontal direction.
3) On the contrary, the HTO diffusion experiments showed that D_e and φ for vertical direction in the Wakkanai formation was smaller than their values for horizontal direction.
4) The τ estimated from 3D image analysis was roughly isotopic for vertical and horizontal directions. This was consistent with the δ/τ^2 obtained from HTO diffusion experiments for vertical and horizontal directions in the Wakkanai formation.
5) The number of start face voxels connected to end face to the Z direction was less than the one to other directions. This result was consistent with the results from the diffusion experiments that the φ for vertical direction in the Wakkanai formation was smaller than their values for horizontal direction. This agreement indicated that the number of effective diffusion path correlated with φ.
6) The δ and its distribution were provided using the 3D image describing the sub-micron sized features present in many siliceous mudstone samples. The δ/τ^2 value obtained from HTO diffusion experiments was much larger than the δ/τ^2 value, 0.07 from 3D image analysis but was close to the $1/\tau^2$, 0.15. It indicated that the δ could be neglected (equal to 1) and the HTO-diffusion-accessible pore sizes of the siliceous mudstone investigated here were much bigger than the HTO size. These results indicated that the dominant parameters that control diffusion of HTO in the present system are the φ and the τ.

Acknowledgements

"Project for Assessment Methodology Development of Chemical Effects on Geological Dispossal System" funded by Ministry of Economy, Trade and Industry of Japan. We thank Toshiyuki Nakazawa and Norikazu Yamada (Mitsubishi Materials Corporation-Japan) for their technical support to this project.

References

[1] T. B. Boving, P. Grathwohl, J. Contam. Hydrol., 53 (2001) 85-100.
[2] Bear, J., Dynamics of fluids in porous media, Dover Publ., New York, 1972.
[3] J. A. Currie, Brit. J. Appl. Phys. 11 (1960) 318-324.
[4] W.B. Lindquist, S. Lee, J. Geophys. Res., 101 (1996) 8297-8310.
[5] W.B. Lindquist, A. Venkatarangan, Phys. Chem. Earth, A 25 (1999) 593-599.
[6] C. Shackelford, J. Contam. Hydrol., 7 (1991) 177-217.
[7] J.H. Wang, C.V. Robinson, I.S. Edelmans, J. Am. Chem. Soc. 75 (1953) 466–470.
[8] P. Delage, G. Lefebvre, Can. Geotech. J., 21 (1984) 21-35.
[9] V. Clausnitzer, J.W. Hopmans, Adv. Water Resour. 22 (1999) 577-584.